Simulating electron momentum spectra of *iso*-$C_2H_2Cl_2$: A study of the core electronic structure*

Huang Yan-Ru(黄艳茹)† and Chen Ming-Ming(陈明明)

Department of Physics, Liaoning Shihua University, Fushun 113001, *China*

(Received 13 June 2013; revised manuscript received 2 July 2013; published 12 November 2013)

Electron momentum spectroscopy (EMS) has been used for the first time to study core electronic structure of *iso*-$C_2H_2Cl_2$. In the present work, the pronounced difference between ionization energies of two C_{1s} core orbitals ($2A_1$ and $3A_1$) is seen as a chemical shift of 3 eV, which is due to different chemical environments of the related carbon atoms. Both the calculated spherically averaged core electron momentum distributions (MDs) and three-dimensional electron momentum density maps show that these core molecular orbitals (MOs) $2A_1$ and $3A_1$ exhibit strong atomic orbital characteristics in real and momentum space. However, the core states $2B_2$ and $4A_1$, which are almost degenerate and related to two equivalent atoms, exhibit notable differences between the momentum and position depictions. In contrast to the position space, the momentum density maps of these two core MOs highlight the interference effects which are due to the nuclear positions. The $2B_2$ orbital of *iso*-$C_2H_2Cl_2$ is the antisymmetric counterpart of the $4A_1$ core orbital in real space. However, it relates to the $4A_1$ orbital by an exchange of maxima and minima in momentum space. Due to interference effects between electrons scattered from different atomic centers, modulations with a periodicity of 1.12 a.u. can be seen in the computed momentum densities, which tend to decay with increasing electron momenta. Accordingly, the EMS can not only effectively image the electronic structure of compounds by studying valence orbitals, but also provides direct information on the nature of the nuclear geometry by investigating the core states.

Keywords: (e, 2e) reaction, chemical shift, momentum distributions, core orbitals

PACS: 31.15.–p, 31.15.xr, 33.15.–e **DOI:** 10.1088/1674-1056/23/1/013101

1. Introduction

Electron momentum spectroscopy (EMS), based on a binary (e, 2e) single electron ionization, is a uniquely powerful theoretical and experimental tool of obtaining information about the electronic structure of matter, atoms, and molecules.[1–9] It has been known as an informative experimental method for direct and precise measurements of the ionization energy spectrum. It determines orientationally averaged orbital momentum densities corresponding to individual ionic states. In the (e, 2e) electron impact ionization reaction, an incident electron of energy E_0 causes the single electron ionization of the target system. The EMS kinematics can be completely determined by detecting the two outgoing scattered electrons in coincidence, with energies E_1 and E_2, polar angles θ_1 and θ_2, and a relative azimuthanl angle ϕ. The suitable experiment configuration used in this present work is the symmetric non-coplanar geometry in which cross sections are measured for scattering at equal energies ($E_1 = E_2$) with equal polar angles ($\theta_1 = \theta_2 = 45^\circ$) and a varying relative azimutal angle ϕ.

Within the plane wave impulse approximation (PWIA), the binary encounter approximation, and the target Hartree–Fock or Kohn–Sham approximation,[1,10] the differential EMS cross sections for randomly oriented molecules at gas phase are given by[10]

$$\sigma_{\mathrm{EMS}} \propto \int |\varphi_\alpha(\boldsymbol{p})|^2 \mathrm{d}\Omega, \tag{1}$$

where $\boldsymbol{p}$ is known as the momentum of the target electron at the instant of ionization, and $\varphi_\alpha(\boldsymbol{p})$ is the Fourier transform of the real representation orbital wavefunction $\varphi_\alpha(\boldsymbol{r})$. The quantity $\mathrm{d}\Omega$ gives the spherical average over the random orientations of the target molecules.

The core MO energies are calculated using *ab initio* Hartree–Fock (HF) and density functional theory (DFT) in conjunction with the nonlocal hybrid and gradient corrected Becke-three-parameter Lee–Yang–Parr functional (B3LYP)[11,12] and Dunning's correlation consistent polarized valence basis set of triple-ξ quality basis set augmented by a set of diffuse {s, p} functions on the hydrogen atoms together with a set of diffuse {s, p, d} functions on the carbon and chlorine atoms (aug-cc-pVTZ).[13]

Chemists usually concentrate on valence shells[14–20] or the frontier MOs[21,22] for chemical bonding mechanisms not only because they are more accessible to experimental observation but also because of their importance to chemical processes, and the theoretical interest in calculating SCF wavefucntions and many-body effects.[23–25] Moreover, this is true for most cases in chemical science since the core states show very strong atomic characteristics in various chemical envi-

*Project supported by the National Natural Science Foundation of China (Grant No. 11074144).

†Corresponding author. E-mail: hyr04@mails.tsinghua.edu.cn

© 2014 Chinese Physical Society and IOP Publishing Ltd

ronments. However, core orbitals do also exhibit properties of theoretical and practical significance, which makes their studies worthwhile. Splitting of core levels through spin–orbit and exchange interactions, and so-called chemical shifts induced in core binding energies by the molecular or crystal environment, have already been exploited in electron spectroscopy for chemical analysis (ESCA) spectra to deduce some information about chemical dynamics.[26–30] The measurement of core electron momentum distributions through EMS can be expected to provide richer details than the observation of binding energies alone, as has been demonstrated by direct observations of the chemical shift and electron momentum distributions of core shell in N_2O.[31] In momentum space, core orbitals are rich in information on molecular geometry and orientations. This promises to be a fruitful area of research, in particular in studying the properties of molecules on surface, because interference phenomena have been of crucial importance in the foundation of quantum mechanics. Cohen and Fano[32] predicted by using a simple model that the spectrum of photoelectrons emerging from diatomic molecules is modulated by interferences. It has been reported that EMS can show interference effects in diatomic molecules such as H_2[1] and N_2.[26]

As in the simpler cases of unsaturated hydrocarbon molecules with a single C=C double bond, ethylene and its derivatives including vinyl halides, dimethyl-substitutes, and dihalo-substitutes have been focused on.[33–36] Investigating the electronic structure of these molecules help to understand the effects of ligand substitution and isomeric changes on the C=C bonding morphology. In particular, by comparing the high-resolution He-I, and He-II photoelectron spectra of *cis*-, *trans*-, and *iso*-dichloroethylene isomers, it has been demonstrated that the valence-shell features of these isoelectronic series are similar.[37–40] In addition, in the photoelectron investigation performed with monochromatic synchrotron radiation at a photon energy of 120 eV, Ying and Leung[41] have observed the extensive many-body states of these isomers in the inner-valence region, which can be referred to as breakdown of the orbital picture of ionization in the inner valence region. Cederbaum and his co-workers have studied in details this general phenomenon, and their famous studies[42–44] support the view that the independent particle or orbital picture of ionization most often breaks down in the inner-valence region. The electronic structure and reactivity of these molecules are also of practical interest to the synthesis of conducting polymeric materials. Gorunganthu *et al.*[33] discussed the MDs of the highest occupied molecular orbitals in ethylene and vinyl halides in 1989. The theoretical and experimental investigation of MDs of valence-shell ionic states of the geometric isomers of dichloro-substituted ethylene, i.e., *iso*, *cis*, and *trans* isomers of dichloro-substituted ethylene, have been reported previously.[45–47] The general features of the complex structure observed in the inner valence region in these studies on the valence-shell electron MDs indicate the need for more elaborate quantum chemistry calculations that take into account of electron final or initial–final state correlation effects. It should be noted that core ionization is also subject to a dispersion of the ionization intensity into shake-up states. Although this problem is less acute than for the inner-valence region, it should not be ignored. The famous papers[48–50] by Dobrodey, Cederbaum, and Tarantelli using Green's function explain that a phenomenon of partial localization of core holes, which leads to distinct interference effects in X-ray photoelectron spectra. In this work, we want to find this distinct interference effects in the electron momentum distributions of core orbitals of *iso*-$C_2H_2Cl_2$, so the relativistic effects have been ignored. However, it should be stated that due to the interaction among electrons and the spin–orbital interaction, relativistic effects at low moments and for valence orbitals of heavy elements cannot be neglected. References [51] and [52] indicated that relativistic effects have significant influences on the momentum distributions for valence orbitals of I_2 and Au_2.

Although EMS is a well-established and successful probe of the valence-shell electronic structure of a wide range of atomic and molecular targets, it has seldom been applied to core states because of the weakness of the cross section in the core region. The observed binding energy value interval between two C_{1s} core MOs of *iso*-dichloroethylene is approximately 3 eV,[48–50] so with a high performance electron momentum spectrometer, EMS measurements upon these core levels may be foreseen in the near future. Hence, the EMS studies of core orbitals for *iso*-$C_2H_2Cl_2$ at this time can only rely on theoretical electronic structure in momentum space. To our knowledge, it is the first global study of core orbitals MDs of *iso*-$C_2H_2Cl_2$, as it has never been studied previously either theoretically or experimentally.

2. Results and discussion

2.1. Core orbital ionization energy

Iso-dichloroethylene belongs to the symmetry point group C_{2v} and the principal C_2-rotational axis is the z axis, its reflection plane is yz plane. The core orbitals of ground state electronic configuration of *iso*-$C_2H_2Cl_2$ can be written as

$$\cdots(2A_1)^2(3A_1)^2(2B_2)^2(4A_1)^2\cdots.$$

Since core MOs usually have atom-localized electronic states, the binding energies and orbitals of the core electrons are element specific in the core region. Figure 1 demonstrates that in position space, the electron density appears atomic-like, the electrons being concentrated very close to the corresponding nuclei with essentially no density between them. The core

MOs $2A_1$ and $3A_1$ of *iso*-$C_2H_2Cl_2$ are centered at the (right) carbon atom labeled by C_R (see Fig. 1(a)), at the side of the chlorine atoms, and the other (left) carbon atom labeled by C_L, at the side of the hydrogen atoms (see Fig. 1(b)), respectively. From the other side, the $2B_2$ orbital is the antisymmetric counterpart of $4A_1$ core orbital. These core orbitals consist primarily of the 2s orbitals of chlorine, being either out of phase ($2B_2$, Fig. 1(c)) or in phase ($4A_1$, Fig. 1(d)), in a position space perspective. Details of all core MOs binding energies of *iso*-dichloroethylene and the atomic orbital energies of carbon and chlorine atom are shown in Table 1.

As shown in Table 1, the binding energies of the four core orbitals of *iso*-dichloroethylene are higher when ΔB3LYP is used, compared to OE (B3LYP) and SAOP. However, the energy differences between the $2A_1$ and $3A_1$ states, as well as the degenerate core MOs $2B_2$ and $4A_1$ are in agreement with three theoretical calculations. After the careful examination of all the core orbital energies of the two carbon atoms, it is noticed that the calculated results underestimate the experimental ones. However, the energy trends for the C_R and C_L are the same in the ΔB3LYP, OE (B3LYP), and SAOP calculations: C_R exhibits larger core MO energies than C_L. As can be seen from Table 1, the binding energy of MO $2A_1$ overestimates that of MO $3A_1$ by about 3.0 eV due to the electronegativity of the chlorine atoms. This difference in energy level is linked with the chemical shift observed in ESCA spectra,[30] which originates from different chemical environments which surround the two nuclei C_R and C_L. For the core states of the 2s orbitals of the chlorine atoms, which have an analogous surrounding except that the $2B_2$ orbital is out of phase and the $4A_1$ is in phase, the binding energies are nearly degenerate. With present-day techniques, it is impossible to resolve them.

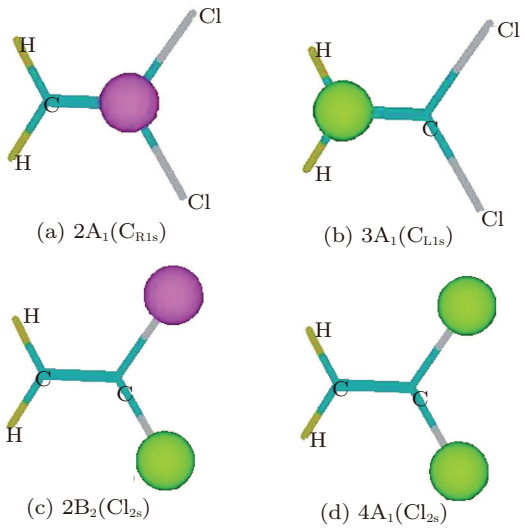


Fig. 1. (color online) Core orbital electron density maps of *iso*-$C_2H_2Cl_2$ in position space. (a) $2A_1$ (C_{R1s}), (b) $3A_1$ (C_{L1s}), (c) $2B_2$ (Cl_{2s}), and (d) $4A_1$ (Cl_{2s}).

Table 1. The experimental and theoretical vertical ionization potentials (eV) of C_{1s} orbitals of the three molecules (C_2Cl_4, *iso*-$C_2H_2Cl_2$, and C_2H_4) and Cl_{2s} orbitals of *iso*-$C_2H_2Cl_2$ together with the C_{1s} orbital of isolated C atom and Cl_{2s} orbital of isolated Cl atom are showed. Three types of theoretical calculations (ΔB3LYP, OE, SAOP)[53,54] are conducted with the ADF program for each orbital of every molecule. The magnitude of orbital energy is abbreviated to OE. TZ2P basis sets are employed throughout the calculation.

	Orbital	Expt.[a)]	ΔB3LYP	OE(B3LYP)	SAOP
C-atom	1s		298.65	281.56	277.00
C_2Cl_4	$2A_g$	293.64	289.24	280.67	276.79
	$2B_{1u}$	293.64	289.22	280.64	276.77
iso-$C_2H_2Cl_2$	$2A_1$	293.62	290.64	280.22	276.50
	$3A_1$	290.93	287.76	277.41	273.83
C_2H_4	$1A_g$	290.7	286.59	276.94	273.49
	$1B_{1u}$	290.7	286.57	276.92	273.47
Cl-atom	2s		269.11	258.53	253.25
iso-$C_2H_2Cl_2$	$2B_2$	277.90	263.57	257.96	252.40
	$4A_1$	277.90	263.57	257.96	252.40

[a)] Refs. [48]–[50].

Due to the similarities in geometries and double bond frames of ethylene, tetrachloroethylene and *iso*-dichloroethylene, we can use the C_{1s} core orbital in either C_2H_4 or C_2Cl_4 as benchmarks to discuss the chemical shift between two nonequivalent carbon atoms, C_R and C_L, of *iso*-$C_2H_2Cl_2$ molecule. Table 1 also lists the ionization energies of the core orbitals of C_2Cl_4 and C_2H_4.

As shown in Fig. 1(a), C_R interacts with the two chlorine atoms and the carbon atom through the C_L=C_RCl_2 skeleton in *iso*-$C_2H_2Cl_2$, which can be easily compared with the analogous C_L=C_RCl_2 one in C_2Cl_4, except that C_R and C_L are not equivalent in *iso*-$C_2H_2Cl_2$ (with H_2C_L=C_RCl_2). Thus, the C_{1s} core orbital of C_R in *iso*-$C_2H_2Cl_2$ behaves more like the C_{1s} core orbital of C_2Cl_4. However, the C_{1s} core orbital of C_R in *iso*-$C_2H_2Cl_2$ is marked by a slight drop in ionization energy due to the bonding with H_2C_L. Furthermore, the ionization energy of C_L is smaller for the C_{1s} core orbital in ethylene (C_2H_4) due to the interaction with the two hydrogen atoms and the carbon atom. The two chlorine atoms on the right-hand side lift the binding energy of the C_{1s} core orbital of C_L in *iso*-$C_2H_2Cl_2$. As can be seen in the orbital correlation diagram for C_2Cl_4, *iso*-$C_2H_2Cl_2$, and C_2H_4 (Fig. 2), the energies of the

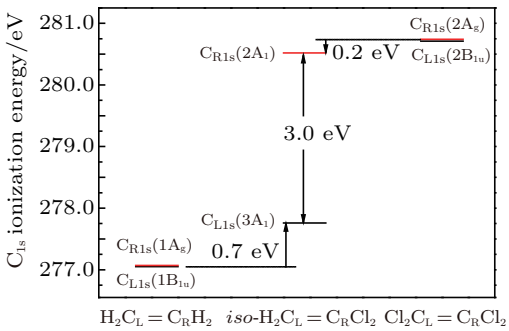


Fig. 2. (color online) The core orbital energy correlation diagram for C_2H_4, *iso*-$C_2H_2Cl_2$, and C_2Cl_4, based on the B3LYP/aug-cc-pVTZ functions.

C_{1s} core orbitals indicate that the molecular environmental effects on chemical shifts can be observed, similar to the cases of *n*-butane,[28] N_2O,[31] and some bicyclic hydrocarbons.[55]

Since the two chlorine atoms are equivalent in *iso*-dichloroethylene, the core $2B_2$ and $4A_1$ MOs, which are dominated by contributions from these atoms, are energetically degenerate, as can be seen in Table 1.

2.2. Momentum distributions of core orbitals

2.2.1. MOs $2A_1$ and $3A_1$

From the maps of the electronic density distributions in coordinate space for the two core $2A_1$ and $3A_1$ MOs of *iso*-dichloroethylene, which are given in Figs. 1(a) and 1(b), it is clear that each core MO has considerable contributions from one-atom states. The electron density distributions of the $2A_1$ and $3A_1$ orbitals exhibit dominant contributions from C_{1s}-atom orbitals of the two non-equivalent carbon atoms C_R and C_L. As a consequence, $2A_1$ ($\psi^{MO} \approx c\phi_{C_R}^{AO}$) and $3A_1$ ($\psi^{MO} \approx c\phi_{C_L}^{AO}$) are non-bonding. Moreover, the spatial charge distribution is the same in both $2A_1$ and $3A_1$ core MOs, showing pure spherical distributions of the C_{1s} atom orbital. As a result, three-dimensional density maps and the momentum profiles of two core MOs wave functions in Figs. 3(a)–3(f) and figure 4 exhibit clearly s-symmetry, i.e., the momentum distribution has a maximum at $p = 0$ and decreases with increasing momentum. It stresses the non-bonding C_{1s} atomic orbital character, even though these two carbon atoms experience significant shifts in core molecular orbital ionization energy as the orbital center moves from C_R to C_L. Moreover, both core orbitals $2A_1$ and $3A_1$ almost coincide in momentum space. The observed limited difference is situated only in the small momentum regions of the momentum density maps and momentum profiles.

Finally, the two C_{1s} core molecular orbitals in *iso*-$C_2H_2Cl_2$ exhibit distinctly different orbital energy and bear a large chemical shift of about 3 eV between core orbitals $2A_1$ and $3A_1$, as revealed in Table 1 and Fig. 2. On the contrary, in momentum space, the corresponding C_{1s} orbitals are almost indistinguishable and the orbital momentum distributions of $2A_1$ and $3A_1$ are nearly identical (see Figs. 3(a)–3(f) and Fig. 4).

2.2.2. MOs $2B_2$ and $4A_1$

Any molecular orbital, including the normalized Dyson orbital $\varphi_\alpha(\boldsymbol{r})$, can be represented as a sum of terms of centered at each equilibrium nuclear position $\boldsymbol{R}_s$, i.e., a linear combination of atomic orbitals,

$$\varphi_\alpha(\boldsymbol{r}) = \sum_s \xi_\alpha^{(s)}(\boldsymbol{r} - \boldsymbol{R}_s). \tag{2}$$

In expression (2), $\boldsymbol{r}$ is the radial coordinate of the electron, and α labels the symmetry manifold and the orientation of the orbital. The normalized Dyson orbital in momentum space can be written as

$$\begin{aligned}\varphi_\alpha(\boldsymbol{p}) &= (2\pi)^{-3/2}\int \mathrm{d}^3\boldsymbol{r}\exp(-\mathrm{i}\boldsymbol{p}\cdot\boldsymbol{r})\,\varphi_\alpha(\boldsymbol{r}) \\ &= \sum_s (2\pi)^{-3/2}\int \mathrm{d}^3\boldsymbol{r}\exp(-\mathrm{i}\boldsymbol{p}\cdot\boldsymbol{r})\,\xi_\alpha^{(s)}(\boldsymbol{r} - \boldsymbol{R}_s) \\ &= \sum_s \eta_\alpha^{(s)}(\boldsymbol{p})\exp(-i\boldsymbol{p}\cdot\boldsymbol{R}_s),\end{aligned} \tag{3}$$

where $\eta_\alpha^{(s)}(\boldsymbol{p})$ is atomic orbital in the momentum space, and

$$\eta_\alpha^{(s)}(\boldsymbol{p}) = (2\pi)^{-3/2}\int \mathrm{d}^3\boldsymbol{r}\exp(-\mathrm{i}\boldsymbol{p}\cdot\boldsymbol{r})\,\xi_\alpha^{(s)}(\boldsymbol{r}). \tag{4}$$

The position origin is translated to $\boldsymbol{R}_s$ for each integrand. As can be seen from expressions (2) and (3), there is a major difference between the coordinate and momentum representations. The momentum–space atomic orbitals all have a common center at the origin of momentum space. The information about the nuclear geometry structure is carried rather subtly in the form phase factor. There are no bond lengths in $\boldsymbol{p}$ representation as there are in coordinate space, the molecular geometry manifests itself through bond oscillations due to the interference terms in the momentum space molecular wavefunctions. The phases and hence interference terms have a small effect for $p \propto 1/R_{st}$, with R_{st} being the distance between atoms s and t. However, bond oscillations are much more noticeable in the inner valence and core orbitals. Comparing Figs. 1(c) and 1(d) with Figs. 3(g)–3(l) and Fig. 4, bond oscillations are extended in momentum space whereas they are highly localized in position space. It is noted that the outer-valence orbitals are in turn more localized in momentum space but diffuse in position space.

When $\varphi_\alpha(\boldsymbol{r})$ has two or more cusps or local extrema separated by $\boldsymbol{R}_{st}$, it follows from Eqs. (2) and (3) that a sinusoidal modulation with a period $T_p = 2\pi/R_{st}$ and along a direction $\boldsymbol{R}_{st}$ is introduced into the momentum density through a phase factor $\exp(-\mathrm{i}\boldsymbol{p}\cdot\boldsymbol{R}_s)$. This preserves the nuclear geometry information, since $\varphi_\alpha(\boldsymbol{r})$ will usually have a cusp at each nucleus. The amplitude of this modulation is maximal for linear molecules of high symmetry when these local extrema are clearly pronounced relative to the rest, which has also been seen in the case of the N_2 molecule.[26] The phase of this modulation depends on the symmetry, bonding character, and nodal structure of the molecular orbital. Along $\boldsymbol{p}$ and parallel to $\boldsymbol{R}_{st}$, the momentum density is either increased or decreased, according to $P = n\pi/R_{st}$ and becomes progressively weaker with increasing n. As a result, due to two or more equivalent nuclei in each molecule, quantum superposition of the identical essentially atom-like core wave function $\xi_\alpha^{(s)}(\boldsymbol{r} - \boldsymbol{R}_s)$ on these centers $\boldsymbol{R}_s$ produces the evident periodically multipeaked momentum distributions in the momentum density maps, which do not exist in the momentum density maps of valence orbitals. The spacing of maxima is determined solely by the internuclear distances. The resulting interference largely disappears in the final spherical average.

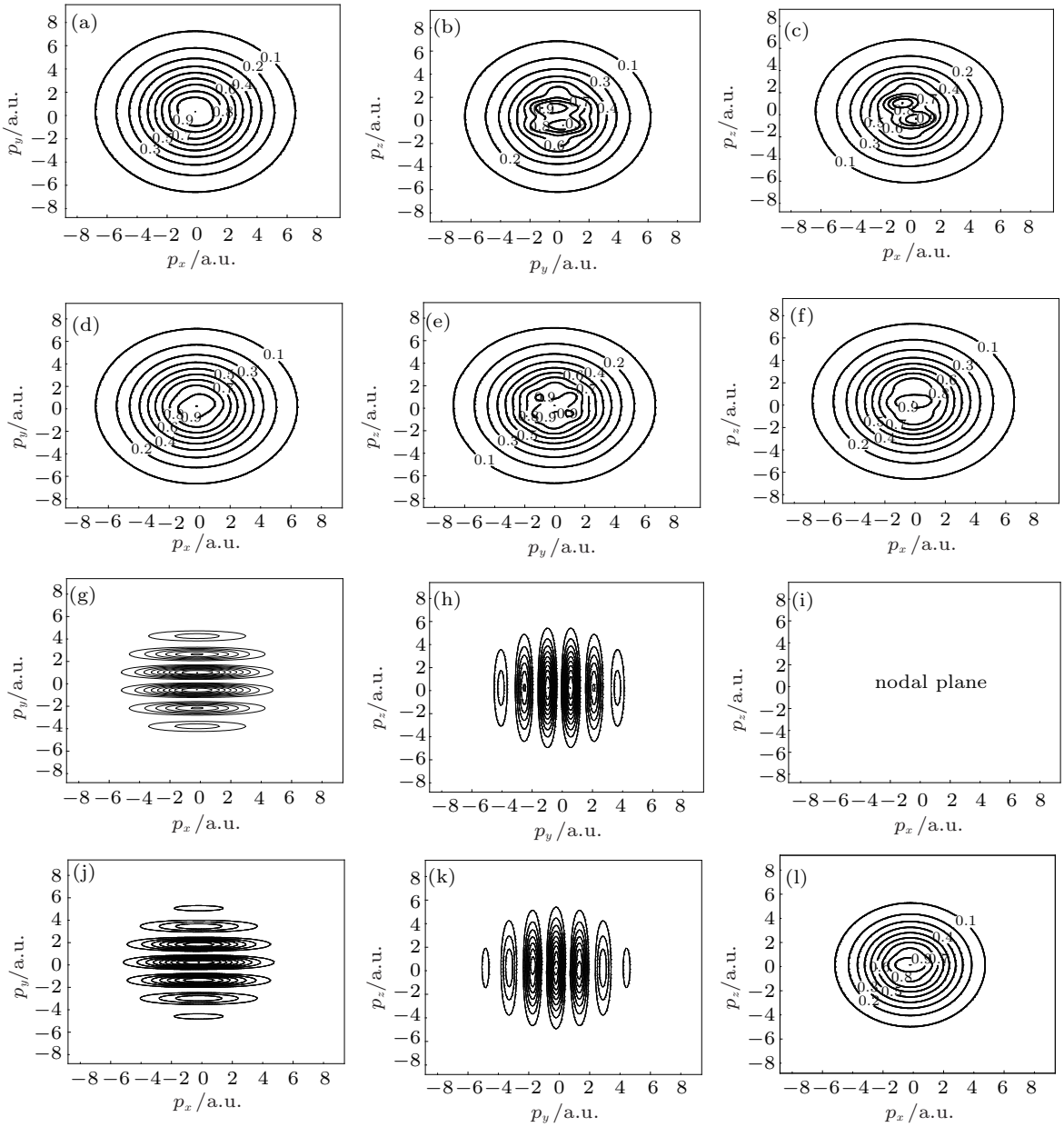


Fig. 3. DFT-B3LYP/aug-cc-pVTZ calculated three-dimensional momentum distribution maps for core states of *iso*-$C_2H_2Cl_2$ in the momentum representation. (a) $p_x - p_y$ plane for $2A_1$ orbital, (b) $p_z - p_y$ plane for $2A_1$ orbital, (c) $p_z - p_x$ plane for $2A_1$ orbital, (d) $p_x - p_y$ plane for $3A_1$ orbital, (e) $p_z - p_y$ plane for $3A_1$ orbital, (f) $p_z - p_x$ plane for $3A_1$ orbital, (g) $p_x - p_y$ plane for $2B_2$ orbital, (h) $p_z - p_y$ plane for $2B_2$ orbital, (i) $p_z - p_x$ plane for $2B_2$ orbital, (j) $p_x - p_y$ plane for $4A_1$ orbital, (k) $p_z - p_y$ plane for $4A_1$ orbital, and (j) $p_z - p_x$ plane for $4A_1$ orbital.

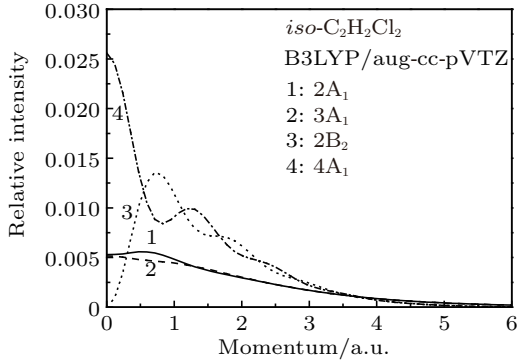


Fig. 4. The theoretical spherically averaged orbital electron momentum distribution.

The $2B_2$ orbital in Fig. 1(c) has two out of phase atomic centers and is thus antisymmetric along the y axis. As a result of the mechanisms discussed above, the momentum density contour maps on p_xp_y and p_yp_z planes in Figs. 3(g) and 3(h) show marked interference effects. The momentum distribution map of this orbital is periodic along p_y. According to the optimized B3LYP/aug-cc-pVTZ molecular geometry of *iso*-$C_2H_2Cl_2$, the distance between the chlorine atoms is about 2.96 Å. Thus, whereas the momentum densities tend overall to decrease with increasing electron momenta, they exhibit a modulation with a periodicity $T_p = 2\pi/R_{st} \approx 1.12$ a.u. The $2B_2$ orbital is an odd wave function of y; the p_y amplitude vanishes exactly and the p_xp_z plane is a nodal plane (see Fig. 3(i)). We see a strongly multi-peaked structure as a result of interference between the atomic core orbitals centered on the two equivalent chlorine nuclei. The first peak at $p \approx 0.74$ a.u. is

strong and dominates the profile. The second and third peaks are found at approximately 1.80 and 2.89 a.u. Moreover, it is observed that the momentum interval ($\Delta p \approx 1.1$ a.u.) between two peaks is close to the periodicity $T_{\rm p}$. Due to the phase factor $\sum_s \exp(-{\rm i}\boldsymbol{p}\cdot\boldsymbol{R}_s)$ of Eq. (3), the amplitudes of the three peaks decrease as p increases. Therefore, the last peak appears as only a marginal shoulder in the momentum profile. Because of the antisymmetric character of the orbital, the momentum densities vanish at zero electron momenta.

The $4A_1$ orbital (see Fig. 1(d)) exhibits an in-phase relationship between the Cl_{2s} atomic orbitals. The quantum interference between the two chlorine atom centers is again evident in the p_y components of the momentum maps shown by Figs. 3(j) and 3(k). Since the internuclear spacing $R_{\rm st}$ is the same, thus the periodicity of the modulation of the momentum profile by interference effects is again equal to 1.12 a.u. Because of the difference in-phase relationship, it takes the form for the $2B_2$ orbital of an exchange of maxima and minima in the momentum density maps. The spherically averaged momentum profile of the $4A_1$ orbital in Fig. 4 exhibits an intense peak at zero momentum. The minimum at $p \sim 0.74$ a.u. and the secondary peak at $p \sim 1.20$ a.u. almost coincide with the maximum and a second minimum in the momentum profile of the $2B_2$ orbital. From curve 3 in Fig. 4, it is observed that most of the structure is flattened out through the spherical averaging, but remnants of the interference effects due to the nuclear geometry can still be seen.

Finally, from the position electron density maps for the $2B_2$ and $4A_1$ core MOs (see Figs. 1(c) and 1(d)), it is clear that the two-core MOs primarily consist out of the 2s atomic orbitals of the two equivalent chlorine atoms. According to Eq. (3), the core $2B_2$ and $4A_1$ MOs arise as a superposition of chlorine 2s type states with different patterns of phase relationships. Thus, in position space, the electron densities for the two core atomic functions are similar, except for the non-measurable phases of the actual component: in case of the $2B_2$ MO of *iso*-$C_2H_2Cl_2$, the two atomic orbitals on the Cl atoms have opposite phase, whereas they have the same phase in case of the $4A_1$ MO. The electrons concentrate closely to the two chlorine nuclei and there is no charge population between the atoms. Again, the momentum distributions of these two core orbitals are quite different due to phase effects through Fourier transform. The momentum distributions of the $2B_2$ and $4A_1$ orbitals are distorted from the ideal s-like shape in momentum space through space interference interactions of the two chlorine atoms, revealing a strong orbital polarization.

3. Conclusions

The four core MOs of *iso*-dichloroethylene have been discussed through EMS based on the ΔB3LYP, OE(B3LYP), and SAOP calculations. The $2A_1$ and $3A_1$ core orbitals exhibit large energy intervals and could therefore be resolved individually. The chemical shift, which is seen between these two core orbitals in position space, is largely caused by the electronegativity of the chlorine atoms. However, in momentum space there are virtually no changes in the two C_{1s} core orbitals of *iso*-dichlorethylene and the two core MOs are indistinguishable. Both C_R and C_L do not significantly interact with other molecular orbitals in the core region, so they remain atomic orbitals in $\boldsymbol{r}$ and $\boldsymbol{p}$ space. The three-dimensional momentum density maps and distributions for these two core orbitals both reflect their symmetry character and exhibit marked interference effects between the two equivalent chlorine nuclei. Moreover, the momentum densities of two core orbitals change along p_y with a period $T_{\rm p} = 2\pi/R_{\rm st} \approx 1.12$ a.u. The core orbitals $2B_2$ and $4A_1$ are strongly distorted and split significantly in $\boldsymbol{p}$ state, revealing the fact that core orbitals do interact. Our work demonstrates that MDs of core orbitals can reveal the full richness of nuclear position and spacing in the molecules, which is a major advantage of EMS over the use of position wave functions in the study of core orbitals of molecules. In position space, the core electron density appears atom-like, and the electrons are concentrated very close to the nuclei with essentially no electron sharing. In momentum space, the interference effects related to the nuclear position are marked for molecules containing a number of equivalent atoms. Accordingly, EMS can not only effectively image orbital electron densities through measuring the valence shell of molecules, but it can also provide direct information on the nature of the nuclear configuration and interdistances by probing the core.

An EMS study of core MOs for *trans*-$C_2H_2Cl_2$ and *cis*-$C_2H_2Cl_2$ is currently under investigation in our group. The results will be presented in a following paper. Combined with our present (e, 2e) results on the *iso*-$C_2H_2Cl_2$ molecule (with a $H_2C{=}CCl_2$ backbone), these core orbital MDs can be used to investigate the effects of isomeric changes on the core-shell electronic structure of these isomers of dichloro-substituted ethylene. Finally, we hope that the theoretical results reported in this paper will motivate experiments on *iso*-$C_2H_2Cl_2$, in order to make detailed comparisons and thus to give a better understanding of the electronic structure of *iso*-$C_2H_2Cl_2$.

Acknowledgments

The authors want to thank Prof. Ning and Dr. M. Yurun for help.

References

[1] Weigold E and McCarthy I E 1999 *Electron Momentum Spectroscopy* (New York: Kluwer Academic/Plenum Publishers)
[2] Deng J K, Ning C G, Ren X G, Su G L, Zhang S F, Huang Y R, Yang T C and Liu K 2007 *J. Electron. Spectrosc. Relat. Phenom.* **161** 43

[3] Shi L L, Liu K, Luo Z H, Ning C G and Deng J K 2011 *Chin. Phys. B* **20** 13403

[4] Liu K, Ning C G and Deng J K 2010 *Chin. Phys. Lett.* **27** 073403

[5] Ning C G, Zhang S F, Deng J K, Liu K, Huang Y R and Luo Z H 2008 *Chin. Phys. B* **17** 1729

[6] Yang T C, Ning C G, Su G L, Deng J K, Zhang S F, Ren X G and Huang Y R 2006 *Chin. Phys. Lett.* **23** 1157

[7] Zhang S F, Ning C G, Deng J K, Ren X G, Su G L, Yang T C and Huang Y R 2006 *Chin. Phys. Lett.* **23** 583

[8] Deng J K, Li G Q, Huang J D, Wang F, Ning C G, Lu J, He Y, Wang X D, Zhang Y A, Gao H, Wang Y and Zheng Y Y 2002 *Chin. Phys. Lett.* **19** 47

[9] Ren X G, Ning C G, Deng J K, Zhang S F, Su G L, Li B and Chen X J 2005 *Chin. Phys. Lett.* **22** 1382

[10] McCarthy I E and Weigold E 1991 *Rep. Prog. Phys.* **54** 789

[11] Becke A D 1993 *J. Chem. Phys.* **98** 5648

[12] Lee C, Yang W and Parr R G 1988 *Phys. Rev. B* **37** 785

[13] Feller D 1992 *J. Chem. Phys.* **96** 6104

[14] Deleuze M S, Pang W N, Salam A and Shang R C 2001 *J. Am. Chem. Soc.* **123** 4049

[15] Knippenberg S, Huang Y R, Hajgato B, Francois J P, Deng J K and Deleuze M S 2007 *J. Chem. Phys.* **127** 174306

[16] Ning C G, Luo Z H, Huang Y R, Hajgató B, Morini F, Deng J K and Deleuze M S 2008 *J. Phys. B* **41** 175103

[17] Ning C G, Hajgató B, Huang Y R, Zhang S F, Knippenberg S, Deng J K and Deleuze M S 2008 *Chem. Phys.* **343** 19

[18] Chen X J, Yang G O, Jia C C, Peng L L, Xu C K, Tian S K and Xu K Z 2000 *J. Electron. Spectrosc. Relat. Phenom.* **107** 273

[19] Chen X J, Zhou L X, Zhang X H, Yin X F, Xu C K, Shan X, Wei Z and Xu K Z 2004 *J. Chem. Phys.* **120** 7933

[20] Wang F 2003 *J. Phys. Chem. A* **107** 10199

[21] Liu K, Ning C G, Luo Z H, Shi L L and Deng J K 2010 *Chem. Phys. Lett.* **497** 229

[22] Ren X G, Ning C G, Deng J K, Zhang S F and Su G L 2004 *Chem. Phys. Lett.* **397** 82

[23] Huang Y R, Hajgató B, Ning C G, Zhang S F, Liu K, Luo Z H, Deng J K and Deleuze M S 2008 *J. Phys. Chem. A* **112** 2339

[24] Huang Y R, Ning C G, Deng J K and Deleuze M S 2008 *Phys. Chem. Chem. Phys.* **10** 2374

[25] Miao Y R, Ning C G and Deng J K 2011 *Phys. Rev. A* **83** 062706

[26] Bharathi S M, Grisogono A M, Lahmam-bennaani A, Pascual R and Weigold E 1991 *J. Electron. Spectrosc. Relat. Phenom.* **53** 271

[27] Wang F, Larkins F P, Brunger M J, Michalewicz M T and Winkler D A 2001 *Spectrochim. Acta Part A* **57** 9

[28] Downton M and Wang F 2004 *Chem. Phys. Lett.* **384** 144

[29] Takahata Y and Chong D P 2003 *J. Electron. Spectrosc. Relat. Phenom.* **133** 69

[30] Siegbahn K, Nordling C, Johansson G, Hedman J, Heden P F, Hamrin K, Gelius U, Bergmark T, Werme L O, Manne R and Baer Y 1969 *ESCA Applied to Free Molecules* (Amsterdam: North-Holland Publishing Company)

[31] Su G L, Ning C G, Deng J K and Wang F 2006 *Chem. Phys. Lett.* **422** 308

[32] Cohen H D and Fano U 1966 *Phys. Rev.* **150** 30

[33] Gorunganthu R R, Coplan M A, Leung K T, Tossell J A and Moore J H 1989 *J. Chem. Phys.* **91** 1994

[34] Ying J F, Zhu H, Mathers C P, Gover B N, Banjavcic M P, Zheng Y Y, Brion C E and Leung K T 1993 *J. Chem. Phys.* **98** 4512

[35] Mathers C P, Ying J F, Gover B N and Leung K T 1994 *Chem. Phys.* **184** 295

[36] Mathers C P, Gover B N, Ying J F, Zhu H and Leung K T 1994 *J. Am. Chem. Soc.* **116** 7250

[37] Kimura K, Katsumata S, Achiba Y, Yamazaki T and Iwata S 1981 *Handbook of He I Photoelectron Spectra of Fundamental Organic Molecules* (New York: Halsted Press) p. 59

[38] von Niessen W, Åsbrink L and Bieri G 1982 *J. Electron Spectrosc. Relat. Phenom.* **26** 173

[39] Katrib A, Debies T P, Colton R J, Lee T h and Rabalais J W 1973 *Chem. Phys. Lett.* **22** 196

[40] Manne R 1974 *J. Electron Spectrosc. Relat. Phenom.* **3** 327

[41] Ying J F and Leung K T 1993 *J. Electron Spectrosc. Relat. Phenom.* **63** 75

[42] Deleuze M S, Giuffreda M G, Francois J P and Cederbaum L S 1999 *J. Chem. Phys.* **111** 5851

[43] Deleuze M S and Cederbaum L S 1999 *Adv. Quantum. Chem.* **35** 77

[44] Deleuze M S, Giuffreda M G, Francois J P and Cederbaum L S 2000 *J. Chem. Phys.* **112** 5325

[45] Mei L, Chuaqui M, Mathers C P, Ying J F and Leung K T 1994 *J. Chem. Phys.* **101** 3558

[46] Mei L, Chuaqui M, Mathers C P, Ying J F and Leung K T 1994 *Chem. Phys.* **188** 347

[47] Jolly W L, Bomben K D and Eyerman C J 1984 *Atom. Data Nucl. Data Tables* **31** 433

[48] Dohrodey N V, Cederbaum L S and Tarahtelli F 1998 *J. Phys. Chem. A* **102** 9405

[49] Dohrodey N V, Cederbaum L S and Tarahtelli F 2000 *Phys. Rev. B* **61** 7336

[50] Dohrodey N V, Cederbaum L S and Tarahtelli F 1998 *Phys. Rev. B* **58** 2316

[51] Liu K, Ning C G and Deng J K 2009 *Phys. Rev. A* **80** 022716

[52] Zhu J S, Deng J K and Ning C G 2012 *Phys. Rev. A* **85** 052714

[53] Miao Y R, Deng J K and Ning C G 2012 *J. Chem. Phys.* **136** 124302

[54] Miao Y R, Ning C G, Liu K and Deng J K 2011 *J. Chem. Phys.* **134** 204304

[55] Wang F 2005 *J. Mol. Struct.* **728** 31